Macromolecules **2003,** *36,* 9851−9858

Polyurethane Adhesive Nanocomposites as Gas Permeation Barrier

Maged A. Osman,[†] Vikas Mittal,[†] Massimo Morbidelli,[‡] and Ulrich W. Suter*[,†]

Department of Materials, Institute of Polymers, and Department of Chemistry and Applied Biosciences, Institute of Chemical and Bioengineering, ETH, CH-8092 Zürich, Switzerland

Received July 25, 2003; Revised Manuscript Received November 2, 2003

ABSTRACT: Adhesive nanocomposites of organically modified montmorillonite (OM) and polyurethane have been synthesized and their permeability to oxygen and water vapor has been measured. The gas permeation through the composites was correlated to the volume fraction of the impermeable inorganic part of the OM. The incorporation of small volume fractions of the platelike nanoparticles in the polymer matrix decreased the gas transmission rate, when the interface between the two heterogeneous phases was properly designed. The oxygen transmission rate decayed asymptotically with increasing aluminosilicate volume fraction and a 30% reduction was achieved at 3 vol %, when the clay was coated with bis(2-hydroxyethyl) hydrogenated tallow ammonium or alkylbenzyldimethylammonium ions. In contrast, coating the clay surface with dimethyl dihydrogenated tallow ammonium ions leads to an increase in the gas transmission rate with augmenting inorganic fraction. This was attributed to a probable change in morphology resulting from phase separation at the interface between the apolar pure hydrocarbon clay coating and the relatively polar PU. The water vapor permeation through the PU nanocomposites was more strongly reduced than oxygen and a 50% reduction was observed at 3 vol % silicate fraction. This was attributed to stronger interactions and hydrogen bonding of the water molecules with the PU matrix as well as to their clustering. Differences in the hydrophobicity of the clay coating influenced the water transmission rate. No spectroscopic evidence could be obtained for a reaction between the hydroxyl groups of the clay organic coating and the isocyanate groups of the prepolymer. A mixed morphology, that is, exfoliated layers and intercalated particles was observed in all composites. WAXRD and TEM gave a qualitative picture of the microstructure of the nanocomposites but no conclusive information. Some of the problems to be solved before a correlation between the nanocomposite properties and their microstructure can be established have been outlined.

Introduction

To meet the rising demands of applications, hybrids of inorganic "functional fillers" and polymeric materials are being continuously developed to combine their constituent's beneficial properties or to induce new ones.[1,2] Particulate filled polymers are often classified in micro- and nanocomposites depending on the dimensions of the phases involved. Nanoparticles often strongly influence the properties of the composites at very low volume fractions. This is mainly due to their small interparticle distances and the conversion of a large fraction of the polymer matrix near their surfaces into an interphase of different properties as well as to the consequent change in morphology. As a result, the desired properties are usually reached at low filler volume fraction, which allows the nanocomposites to retain the macroscopic homogeneity and low density of the polymer. Besides, the geometrical shape of the particles plays an important role in determining the properties of the composites. Consequently, nanocomposites have attracted much scientific and industrial interest in the past decade.[3−6]

Polyurethanes (PU) are a versatile class of polymers that can be efficiently tailored to give a diverse range of products such as foams, coatings, adhesives, fibers, rubbers or thermoplastic elastomers.[7,8] Of special interest are polyurethane adhesives, which are used in producing laminates for food packaging due to their flexibility and wide application temperature range. However, their function in laminates is limited to holding together various polymer films and their contribution to the overall barrier performance of the laminates is meager. Often these laminates consist of a polyolefin foil serving as a humidity barrier and a PET foil, as oxygen barrier, and it would be advantageous if the adhesive can contribute to the barrier performance of the laminate. Besides adding a new value to the adhesive component, this would lead to a reduction in laminate thickness and to savings in materials. A polyurethane gas-barrier can also be used as a coating layer that replaces one of the films in the laminate. Enhancement of the permeation-barrier properties of polymers can generally be achieved by incorporating impermeable platelike particles because the permeant molecules have to wiggle around them in a random walk, thus diffusing through a tortuous pathway.[9−11] Platelike nanoparticles are ideal for this purpose because of their geometrical shape and high aspect ratio, and effective improvements can be obtained at low volume fraction, which allows the composite to retain the optical clarity mostly needed in packaging applications.

Montmorillonite is an expandable dioctahedral smectite with a mean layer charge density of 0.25−0.5 equiv/mol and belongs to the family of the 2:1 phyllosilicates.[12,13] Its particles consist of stacks of 1 nm thick aluminosilicate layers with a regular gap between (interlayer). Each layer consists of a central Al-octahedral sheet fused to two tetrahedral silicate sheets. Isomorphic substitutions of aluminum by magnesium in the octahedral sheet generate negative charges, which are compensated for by alkaline-earth- or hydrated alkali-metal cations. The electrostatic and van

---

* Corresponding author. Telephone: +41 1 6323127. Fax: +41 1 6321096. E-mail: ulrich.suter@sl.ethz.ch.

[†] Institute of Polymers, ETH.

[‡] Institute of Chemical and Bioengineering.

10.1021/ma035077x CCC: $25.00

der Waals forces holding the layers together are relatively weak in smectites and the interlayer distance varies depending on the radius of the cation present and its degree of hydration. As a result, the stacks swell in water and the 1 nm thick layers can be easily exfoliated by shearing, giving platelets with high aspect ratio. Unfortunately, their high energetic hydrophilic surfaces are incompatible with many polymers, whose low energetic surfaces are hydrophobic. However, their inorganic cations can be easily exchanged with organic ions (e.g., alkylammonium) to give organically modified montmorillonite (OM) that does not suffer from this problem.[14,15] In this way, long alkyl chains can be ionically bound to the aluminosilicate surface, which increases the basal-plane spacing (*d* spacing) besides decreasing the surface energy.[16] This improves the wetting, swelling, and exfoliation of the aluminosilicate in the polymer matrix.

Nanocomposites of organomontmorillonite with several thermoplastic and thermoset polymers have been described.[3−6] A few studies on polyurethane nanocomposites, in which the synthesis and mechanical properties were described, have also been reported.[17−24] In contrast to microcomposites, impressive improvements in performance were achieved with a small amount of filler. This was ascribed to the high aspect ratio of the exfoliated montmorillonite layers. However, a method to quantify this value is still missing due to difficulties in accurate determination of the diameter (lateral dimension) of the exfoliated layers. The determination of the effective aspect ratio of the particulates in nanocomposites is even more difficult due to the flexibility of the single aluminosilicate layers leading to their bending and folding during preparation of the composite as observed in many published transmission electron micrographs (TEM).[22,25] Over the years, it became common to divide the OM−composites into intercalated and exfoliated types based on the reflections observed in the detection range of wide-angle X-ray diffraction (WAXRD). However, this classification is arbitrary because the observation of a peak in the diffractogram depends not only on the periodicity but also on other factors, such as the concentration and orientation of the aluminosilicates, and does not exclude the presence of exfoliated part. Its absence also does not exclude the presence of small or randomly oriented intercalated particles and therefore, does not indicate complete exfoliation as often postulated.[26−28] There is no doubt that exfoliated layers and intercalated stacks can be present in nanocomposites, but a simple description of their morphology as intercalated or exfoliated is far from adequate. In practice, the morphology of nanocomposites falls between these idealized structures, and it is more probable that a broad mixture of these structures is always present in different ratios. A correlation between the increase in *d* spacing and the nanocomposite properties, which are the real goals, also is still missing and it is not clear how large the *d* spacing should be to attain the required high aspect ratio. Another issue, which is also important for the composite properties and is not addressed by the *d* spacing, is the uniform spatial distribution of the particulates in the matrix and their orientation. Indeed, more work has to be done to quantify the degree of exfoliation and to correlate the macroscopic properties of nanocomposites with their microstructure.

Few studies on the permeation-barrier properties of polyurethane nanocomposites can be found in the literature.[29−31] Xu et al.[29] reported that the relative water vapor permeation (P_c/P_0) of a poly(urethane urea)−Cloisite 15A (Southern Clay, dimethyl dihydrogenated tallow ammonium) composite decreased 5-fold at a 6 vol % filler concentration. Chang et al.[30] observed that the oxygen permeation through polyurethane decreased by 50% or 15% at 4 wt % of montmorillonite surface treated with hexadecylammonium or dodecyl trimethylammonium salts, respectively, and by 35% at 4 wt % Cloisite 25A (Southern Clay/dimethyl dihydrogenated tallow, 2-ethylhexylammonium). However the data given in this reference were not normalized to the film thickness, which varied between 10 and 15 μm, so that those numbers could be misleading. Tortora et al.[31] claimed that the water vapor permeation through a polyurethane composite showed a “remarkable decrease” up to 20 wt % OM concentration.

The objective of the present study was to synthesize adhesive polyurethane−OM nanocomposites with high resistance to oxygen and water vapor permeation. It also included the investigation of the effect of the chemical structure of the clay organic-coating as well as the influence of the filler loading on the barrier performance of the composites. The microstructure of the composites was investigated by electron microscopy and X-ray diffraction.

Experimental Section

Materials. The organoclays were supplied by Süd-Chemie (Moosburg, Germany) under the trade names Nanofil 804, Nanofil 32, and Nanofil 15. The inorganic cations of the mineral were exchanged by the supplier with organic ammonium ions. The chemical structure of the organic cations was bis(2-hydroxyethyl) hydrogenated tallow ammonium; alkylbenzyldimethylammonium (benzalkonium), and dimethyl dihydrogenated tallow ammonium respectively, where tallow represents a mixture of long alkyl homologues with octadecyl the most prominent component. A two-component polyurethane adhesive (Liofol UK3640 + Liofol UK6800) consisting of prepolymer and cross-linker was supplied by Henkel (Düsseldorf, Germany). The prepolymer was a ca. 60% solution of a polyester urethane with isocyanate end groups in ethyl acetate, which also contained 1−3% of diphenylmethane-4,4′-diisocyanate. The cross-linker consisted of a mixture of polyetherglycol carrying amino groups (ca. 80−90%) and 3-aminopropyl)triethoxysilane (ca. 10−20%). Tetrahydrofuran (THF) was purchased from Fluka (Buchs, Switzerland). Polypropylene (100 μm thick) and polyamide (15 μm thick) foils with corona-treated surfaces were donated by Alcan Packaging (Neuhausen, Switzerland) and were used as substrates for the PU−nanocomposites.

Nanocomposite preparation. Due to the adhesive nature of the polyurethane system used, no free-standing films of the nanocomposites could be obtained and films were coated on thin polymer films (PP and PA). These substrates were selected on basis of their high transmission rate for the specific permeant so that they would not hinder measuring the permeation through the nanocomposite film. Their surfaces were corona-treated to enhance the adhesion to the PU coating and to the epoxy matrix, in which the samples were embedded before cutting ultrathin sections for TEM investigations.

The required amount of organoclay was added to 30 g of THF and allowed to swell for about 2 h. The suspension was then cooled in an ice bath and sonicated (ultra sound horn) twice at 70% amplitude for 5 min each time with a 5 min pause in between. Higher amplitudes were avoided in order not to break the particles and reduce their aspect ratio. The prepolymer solution (10 g) was mixed with the suspension and the mixture allowed to stand for 2 h, after which the sonication procedure was repeated. The curing agent (0.2 g) was then added and thoroughly mixed with the prepolymer−clay mixture. The mixture was degassed before drawing a film on the PP and PA films with the help of a bar coater (90 μm gap). The coated film was dried for 20 min at normal pressure and 1 h under reduced pressure at room temperature. This was followed by curing under reduced pressure at 40 °C overnight and 4 h at 60 °C. The dry coating was ca. 10 μm thick and its thickness was determined as described below. The substrate films were also coated with unfilled polyurethane.

The inorganic volume fraction of the nanocomposite (V_m), that is the volume fraction of the pristine montmorillonite before modification, was calculated as follows:

$$V_m = \rho_c m_m / \rho_m,$$

Here ρ_c is the density of the composite, m_m is the mass fraction of the nonmodified montmorillonite in the composite, and ρ_m is its density (2.6 g/cm^3).[32] The correct mass fraction of the organic monolayer on the filler (m_{ml}) was obtained from the thermogravimetric analysis (TGA) of the OM by subtracting the mass loss due to moisture desorption and that due to dehydroxylation of the Na−montmorillonite from the total mass loss.[16] Knowing this value, the aluminosilicate mass fraction in the composite can be calculated. The density of the composite (ρ_c) was calculated from that of the unfilled polyurethane (ρ_{PU}), determined as described below, and that of the OM (ρ_{OM}) as follows:

$$\rho_c = \frac{1}{\dfrac{m_{OM}}{\rho_{OM}} + \dfrac{m_{PU}}{\rho_{PU}}}$$

Here m_{OM} is the mass fraction of the OM and m_{PU} is the mass fraction of the polyurethane.

The density of the OM (ρ_{OM}) was analogously calculated from that of the monolayer (assumed to be equivalent to that of octadecanol $\rho_{ml} = 0.81$ g/cm^3) and that of Na montmorillonite as follows:

$$\rho_{OM} = \frac{1}{\dfrac{m_{ml}}{\rho_{ml}} + \dfrac{m_m}{\rho_m}}$$

Thermogravimetric Analysis (TGA). High resolution (Hi-Res) TGA, in which the heating rate is coupled to the mass loss, that is, the sample temperature is not raised until the mass loss at a particular temperature is completed, was performed in an air stream on a Q500 (TA Instruments) in the temperature range 50−900 °C.

Density and Thickness. The density of the substrate films (PP and PA) and the polyurethane was determined by weighing them in air and in ethanol using an analytical balance (Mettler AE 200) and a homemade device similar to the Mettler density kit ME−33360, following the equation

$$\rho = \frac{\rho_{Et} M}{M - M_l}$$

where ρ is the sample density, ρ_{Et} is the density of ethanol, M is the sample mass in air, and M_l is its mass in ethanol.

The thickness of the substrate film (t) was determined by weighing a piece of defined area. For accuracy, the average of five measurements was taken. The thickness of the coating (t_{coat}) was similarly determined as follows:

$$t_{coat} = (M_1 - M_2)/(\rho_c \times \text{area})$$

where M_1 is the mass of the coated film, M_2 is the mass of a substrate film with the same area and ρ_c is the density of the composite.

Gas Permeation. The oxygen transmission rate through PP foils coated with unfilled polyurethane and with the nanocomposites was measured using an OX-TRAN 2/20 ML (Mocon, Minneapolis, MN) at 23 °C, 1 atm and 0% RH. The oxygen transmission rate was normalized with respect to the film thickness. The water vapor transmission rate through PA foils coated with unfilled PU and with the nanocomposites was measured using a PERMATRAN-W 3/31 MG (Mocon, Minneapolis, MN) at 23 °C, 1 atm and 100% RH. The transmission rate was normalized with respect to the film thickness.

The transmission rate through the nanocomposite film was calculated from that of the coated PP or PA foil as follows:

$$t_{tot}/T_{tot} = (t_1/T_1) + (t_2/T_2)$$

where t_i are the film thicknesses and T_i are the normalized transmission rates.[33] An average of four measurements for each sample is reported.

Transmission Electron Microscopy (TEM). The microstructure of the nanocomposites was studied by bright-field TEM using a Zeiss EM 912 Omega microscope. Pieces of the coated film were embedded in an epoxy matrix (Epon 812 + Durcopan ACM 3:4, Fluka) and 50−100 nm thick sections were microtomed with a diamond knife (Reichert Jung Ultracut E). The section surface was sputter-coated with a carbon layer 3 nm thick.

Wide-Angle X-ray diffraction (WAXRD). Wide-angle X-ray diffraction patterns were collected on a Scintag XDS 2000 diffractometer (Scintag Inc., Cupertino, CA) using Cu Kα radiation ($\lambda = 0.154\,06$ nm) in reflection mode. The instrument was equipped with a graphite monochromator and an intrinsic germanium solid-state detector. The samples were step-scanned (step width 0.02° 2Θ, scanning rate 0.12°/min) at room temperature from 1.5 to 10° 2Θ. The (001) basal-plane reflection of an internal standard muscovite ($2\Theta = 8.84°$) was used to calibrate the line position of the aluminosilicate reflections. To determine the peak positions, the diffractgrams were fitted with a split Pearson VII function (diffraction management system software 1.36b).

Infrared Spectroscopy. Infrared transmission spectra of the coated films were collected on a VECTOR 22 FTIR-spectrometer (Bruker Optics Inc, Billerica, MA). The filler powder was mixed with KBr and pressed into a pill.

Results and Discussion

The three OMs used in this study were chosen on the basis of the chemical structure of the organic cations ionically bonded to the clay surface. The ammonium ions of Nanofil 15 were of pure aliphatic hydrocarbon nature, while those of Nanofil 32 comprised an aromatic moiety beside the alkyl chains, which might lead to increased interactions between the filler and the PU matrix or the solvent. Stronger interactions are expected to enhance the swelling of the OM and to increase the interlayer spacing, which allows easier exfoliation on shearing. The cations of Nanofil 804 contain hydroxyethyl moieties beside the alkyl chains, which match the polarity of the PU better than hydrocarbon chains and may react with the isocyanate groups of the prepolymer. This might result in polymer chains tethered to the clay surface, which can expand the interlayer and sterically hinder the collapse of the aluminosilicate layers. Similar “reactive silicates” have been reported to lead to “exfoliated” structures and higher tensile properties in PU−OM composites.[23,24]

The polyurethane nanocomposites described here were synthesized to combine the impermeability of the crystalline inorganic nanoparticles and the tortuous pathway resulting from their geometrical shape with the favorable properties of the polymer. To improve the dispersion of the particles in the polymer matrix, their surfaces were coated with an ionically bound thin organic layer. However, the permeability of gases

Table 1. Inorganic Volume Fraction in the Polyurethane Nanocomposites

m_{OM}, mass fraction	V_m, vol fraction	ρ_c, composite density (g/cm^3)
0.00	0.0000	1.270
0.03	0.0106	1.278
0.04	0.0141	1.281
0.06	0.0213	1.286
0.08	0.0285	1.291
0.09	0.0321	1.294
0.10	0.0358	1.297
0.12	0.0431	1.302
0.15	0.0542	1.311

through this organic layer is expected to be comparable to that of the polymer rather than to that of the aluminosilicate. That is, the permeation-barrier performance of the composite has to be correlated with the impermeable inorganic content of the composite and not with the total OM concentration. Moreover, it is the volume fraction of the aluminosilicate that influences the properties of the composite and not its mass fraction. Therefore, the corresponding aluminosilicate volume fraction in the OM mass fractions used were calculated and given in Table 1.

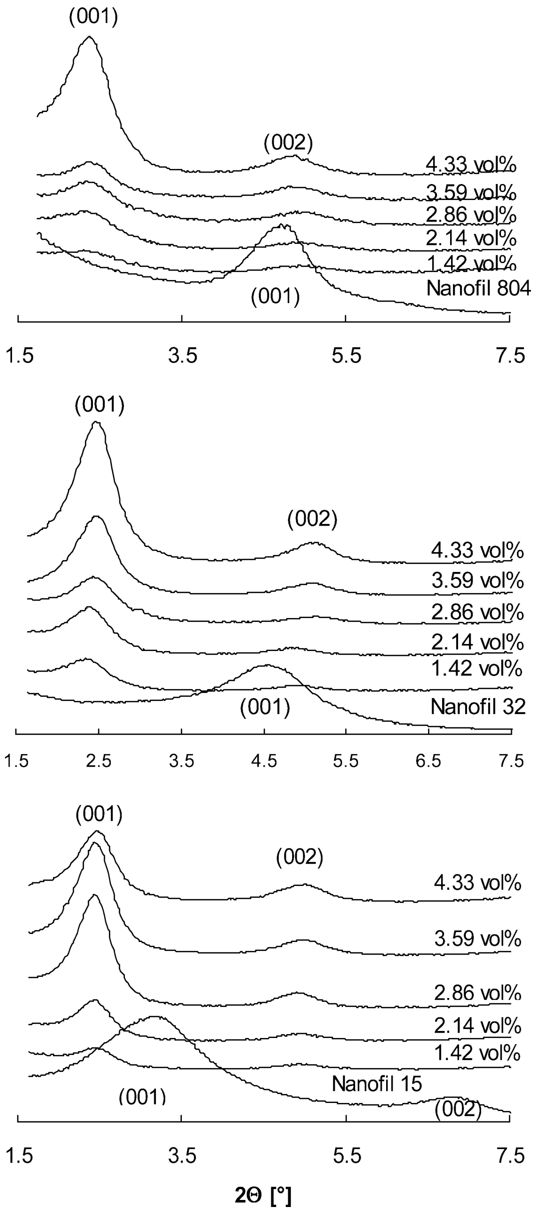

Figure 1. WAXRD patterns of the organically modified clays and their nanocomposites.

The microstructure of all composites prepared was investigated by WAXRD and TEM. The powder diffractograms of the three OMs used are compared to those of the corresponding nanocomposite films in Figure 1. The (001) basal-plane spacing (d_{001}) of the fillers were as follows: 1.85 nm for Nanofil 804, 1.92 nm for Nanofil 32, and 2.74 nm for Nanofil 15, reflecting the differences in thickness of the organic layer between the aluminosilicate layers. In the PU−composites, the interlayer distance calculated from the WAXRD reflections was increased to 3.66, 3.55, and 3.52 nm, respectively, irrespective of the clay concentration. The original basal reflections of the fillers were absent and did not appear with increasing volume fraction, which indicates that the silicate layers did not collapse. The increase in *d* spacing also shows that the polymer was intercalated between the aluminosilicate layers. Although Nanofil 15 had a larger *d* spacing than the other two fillers, the interlayer distance of its composites was comparable to those of the other composites indicating a larger mismatch in the solubility parameters in this case. The TEM micrographs of the 2.86 vol % Nanofil 15 composite (Figure 2) show stacks of parallel layers ca. 4 nm apart (the dark lines represent the aluminosilicate layers). A number of exfoliated single layers as well as double and triple layers randomly oriented can also be seen. Changing the concentration of the filler in the composite did not affect the observed microstructure. The reflection observed in the X-ray difractogram corresponds to the stacks of parallel layers seen in TEM but not to the randomly oriented exfoliated layers. This indicates that the X-ray difractogram does not represent the entire microstructure of the nanocomposite and that a broad mixture of structures extending from single layers to intercalated tactoids is present. Unfortunately, the intensity of the X-ray reflection does not give information on the concentration of the intercalated particles because it strongly depends on the orientation of the platelets. The width of the peak also does not give information on the distribution of the *d* spacing or the particle thickness because of the incomplete orientation and the heterogeneity of the charge distribution in montmorillonite. However, X-ray diffraction has the advantage of giving macroscopic information, while TEM gives local microscopic information only. The general (subjective) impression obtained from TEM was that Nanofil 15 was less exfoliated and intercalated by the PU than the other two fillers. Figure 3 shows TEM micrographs of the 2.86 vol % Nanofil 32 nanocomposite, from which it is obvious that different degrees of intercalation are present beside the exfoliated layers. It can also be seen that the layers are flexible and disordered. Not only the single layers are flexible but also some intercalated stacks of few layers are bent and folded. The general impression is that this filler gives more intercalated tactoids than exfoliated layers. Composites of the same filler containing different volume fractions gave similar TEM micrographs. Although the X-ray diffractograms of the composites of all three fillers look quite similar, we got the impression from the TEM micrographs of the Nanofil 804 nanocomposites (2.86 vol % is shown in Figure 4) that this filler gave more exfoliated layers than the other two. This may be attributed to the presence of hydroxyl groups in the clay organic thin coating, which increases the interaction forces between the filler and the polymer and better

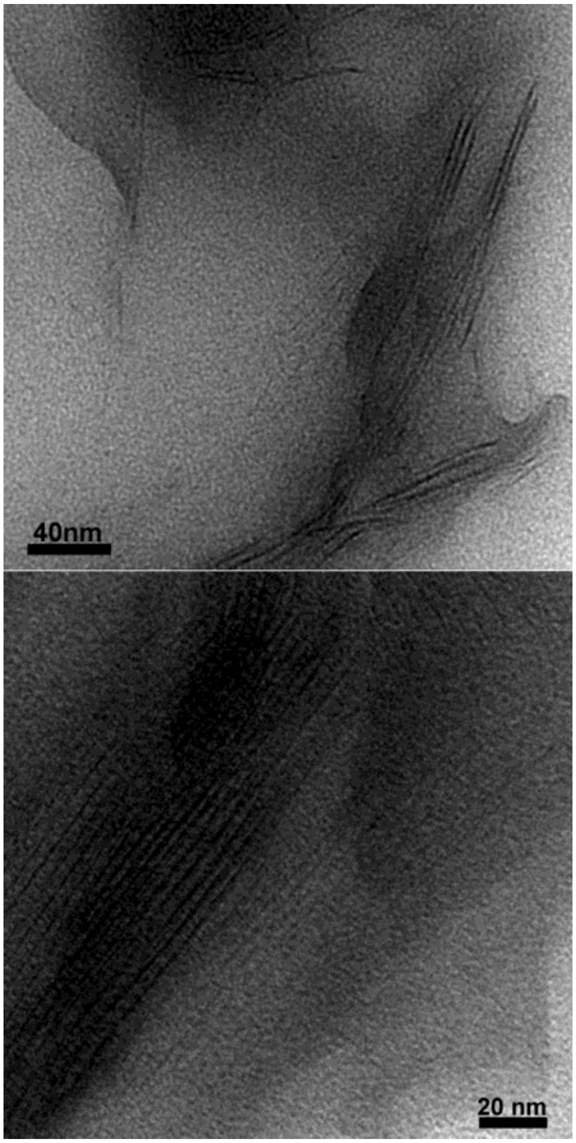

Figure 2. TEM micrographs of the 2.86 vol % Nanofil 15−PU composite.

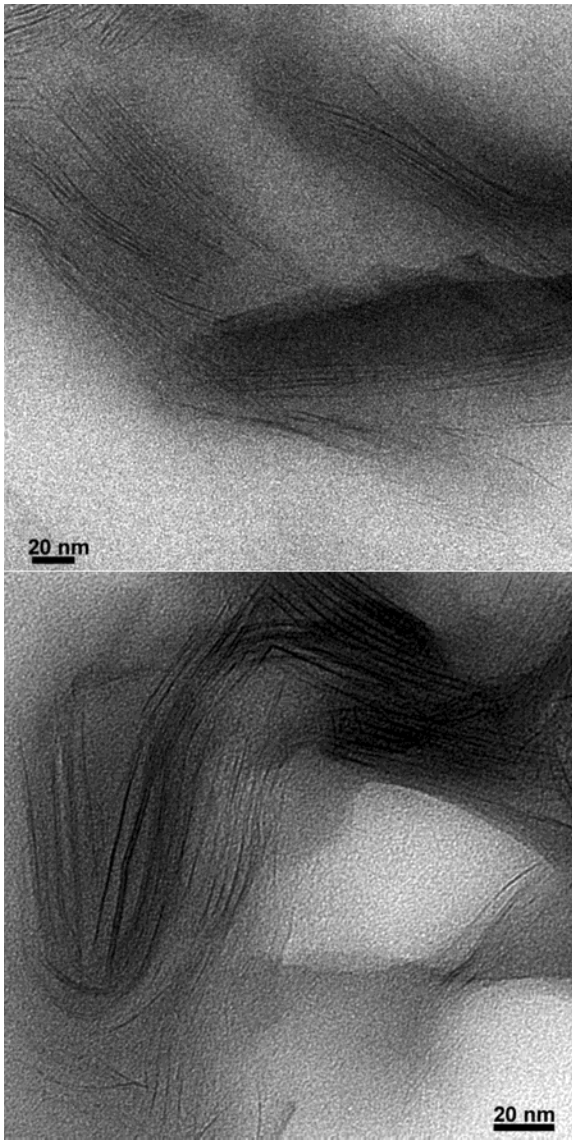

Figure 3. TEM micrographs of the 2.86 vol % Nanofil 32−PU composite.

matches their surface energies. From these results, it can be concluded that the combination of both techniques (TEM and WAXRD) gives a qualitative picture of the microstructure of the nanocomposites but no conclusive information.

It should be remarked that all OMs were strongly swollen in THF, i.e., the particles were expanded “like an accordion” and the layers were separated on sonication. The dispersed layers were well mixed with the polymer components for extended periods of time before driving the solvent off and curing the polymer. In other words, the polymer components were not hindered to enter the interlayer. Despite that, complete exfoliation was not observed after cross-linking the polymer and a part of the filler gave intercalated structures with similar d_{001} for all composites of the different OMs, irrespective of the initial d_{001} of the filler. Very probably equilibrium exists between the attractive forces of the prepolymer molecules and the clay organic coating or the aluminosilicate surface, tending to retain the polymer in the interlayer, and the electrostatic forces between the aluminosilicate layers that tends to squeeze the polymer out. A similar observation has been previously made with Li−montmorillonite.[35] The strength of the electrostatic forces depends on the surface area of the platelets and small particles remain exfoliated, while large ones squeeze a part of the polymer out and give intercalated structures. That is, the broad particle size distribution of the clay leads to a mixture of layers and tactoids of varying thickness. It is not surprising that the attraction forces between the inorganic platelets are partially retained in the organically modified aluminosilicate because the area per cation available on the clay surface is larger than the cross-sectional area of the organic cations present. That is, the aluminosilicate surface is not completely covered by the organic coating and the *d* spacing is not large enough to allow complete decay of the attractive forces between them. In this way a mixed morphology of exfoliated and intercalated structures results.

The oxygen transmission rate through the PU−nanocomposites was measured (Table 2) and plotted relative to that of PU against the silicate volume fraction in Figure 5. For Nanofil 32 and 804, the transmission rate decayed asymptotically with increasing volume fraction so that a 30% reduction in permeability was attained at a filler volume fraction of 3%, while retaining the transparency of the PP foil. The

Figure 4. TEM micrographs of the 2.86 vol % Nanofil 804−PU composite.

Table 2. Oxygen Transmission Rate in PU−OM Nanocomposites (23 °C, 0% RH)

V_m, inorganic vol fraction	oxygen transmission rate (cm^3·mm/m^2·day)		
	Nanofil 804	Nanofil 32	Nanofil 15
0.0000	6.3	6.3	6.3
0.0141	5.0	5.2	7.4
0.0213	4.8	4.7	8.6
0.0285	4.6	4.3	8.6
0.0358	4.6	4.5	9.0
0.0431	4.5	4.3	9.2
0.0542	4.2	4.0	

reduction in transmission rate is obviously a consequence of the tortuous path the gas molecules has to cover during their random molecular motion in order to penetrate the composite film. It should be remarked that the OM platelets are randomly oriented as observed in the TEM micrographs, which reduces their influence on the transmission rate. Fredrickson and Bicerano[10] predicted that, in the dilute regime, poorly oriented platelets are only one-third as effective as aligned ones in reducing the permeability. That is, a stronger reduction in the gas transmission rate can be expected with a coating technique, which leads to better orientation of the platelets. In contrast to the expectation that Nanofil 804 may lead to a better permeation-barrier, the influence of Nanofil 32 and 804 on the transmission rate was similar. A more surprising result was obtained with Nanofil 15, where the transmission rate increased with augmenting filler volume fraction, although no difference in the composite microstructure (TEM and WAXRD) compared to those of the other two filler composites could be observed. This increase in transmission rate must be related to the organic coating of the platelets, since it represents the only difference to the other composites. Since the concentration of the clay coating in the composite is small and the interactions of permanent gases with organic materials are weak, it can only modestly influence the gas solubility in the composite, which cannot be expected to lead to the observed trend reverse. Therefore, it is reasonable to assume that the increase in transmission rate is due to a change in morphology resulting from a phase separation at the interface between the nonpolar hydrocarbon filler coating and the relatively polar PU matrix. This leads to a decrease in density of the organic material (higher free volume) at the interface around the platelets and consequently to an increase in the permeation rate through the composite.[36]

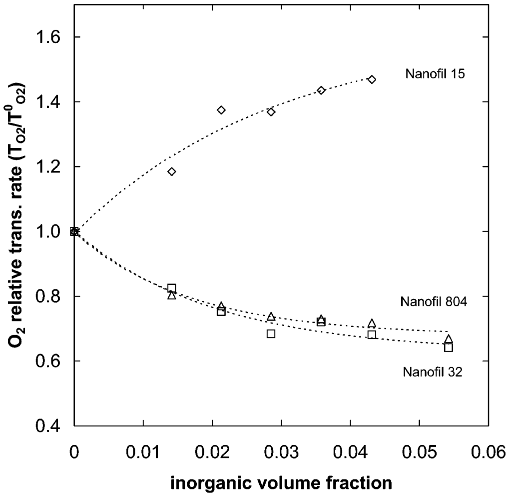

Figure 5. Dependence of the oxygen transmission rate through the PU−nanocomposites on the inorganic volume fraction. The dotted lines are guides for the eye.

It was hoped that the hydroxyl groups of Nanofil 804 can react with the isocyanate groups of the prepolymer and tether polymer chains to the clay surface, leading to more exfoliation or larger *d* spacing and a lower gas transmission rate as often suggested.[23,24] However, WAXRD showed that the *d* spacing of the composite is quite similar to those of the other OM-composites. The oxygen transmission rate of its composites was also quite similar to that of Nanofil 32, which has no possibility to react with the polymer matrix. This provoked us to verify, whether the hydroxyl groups of Nanofil 804 really reacted with the isocyanate groups. IR spectra of the OM and its 2.86 vol % PU−composite as well as that of the unfilled PU are compared in Figure 6. The hydroxyl groups in the organic coating of the clay gave a broad absorption band at 3362 cm^{-1}, whose disappearance in the composite spectrum would indicate their reaction with the isocyanates. Unfortunately, the absorption band at 3345 cm^{-1} due to the NH stretching mode of the polyurethane is relatively broad and is partially superimposed on the OH absorption band. The

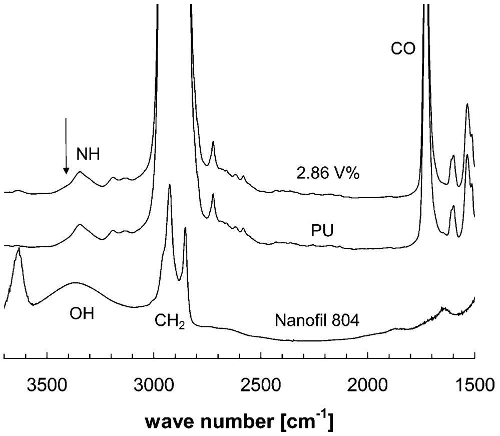

Figure 6. IR spectra of Nanofil 804 and its 2.86 vol % PU−composite compared to that of the unfilled PU.

Table 3. Water Vapor Transmission Rate in PU−OM Nanocomposites (23 °C, 100% RH)

V_m, inorganic vol fraction	water vapor transmission rate (g·mm/m^2·day) Nanofil 804	Nanofil 32	Nanofil 15
0.0000	1.9	1.9	1.9
0.0106	1.4	1.2	1.2
0.0213	1.2	1.1	1.1
0.0321	1.1	1.0	0.9
0.0431	1.0	0.9	0.8
0.0542	0.9	0.7	0.6

OH groups of the cross-linker also did not react completely, and they appear as a shoulder on the NH absorption band in the unfilled PU spectrum. For this reason, the shoulder at ca. 3360 cm^{-1} in the spectrum of the composite does not give conclusive evidence that the OH groups of Nanofil 804 are still present. Consequently, it cannot be said with certainty whether the OH groups of the OM reacted or not. However, in light of the permeation, WAXRD, and TEM results, we are tempted to say that there was little or no reaction. This could be due to deactivation of the OH groups through hydrogen bonding to the aluminosilicate surface or because they were masked by the long alkyl chains.

The water vapor transmission rates through the different PU−nanocomposites are given in Table 3 and are plotted relative to that of PU against the silicate volume fraction in Figure 7. It can be seen that the transmission rate decreases asymptotically with increasing inorganic volume fraction in all the composites and the plateau values are reached at higher filler volume fraction than in the case of oxygen. The decrease in water permeation was also larger than that of oxygen. The transmission-rate decrease in the different composites also reflects the difference in hydrophobicity of the clay coatings. Nanofil 804, whose coating contains hydroxyl groups, showed the least decrease in permeation rate while Nanofil 32, which comprises aromatic moieties, decreased the transmission rate by 50% at a filler volume fraction of 3%. In contrast to the oxygen permeation, no increase in the transmission rate of the water vapor was observed in the case of Nanofil 15 composites. Water molecules are known to associate and build clusters during their diffusion through polymers.[36] This offers a possible explanation for the difference observed in the oxygen and water permeation in this composite. The clusters of water molecules are larger than the oxygen molecules in size and probably cannot travel through the thin gaps resulting from the possible phase separation at the interface between the Nanofil 15 platelets and the PU.

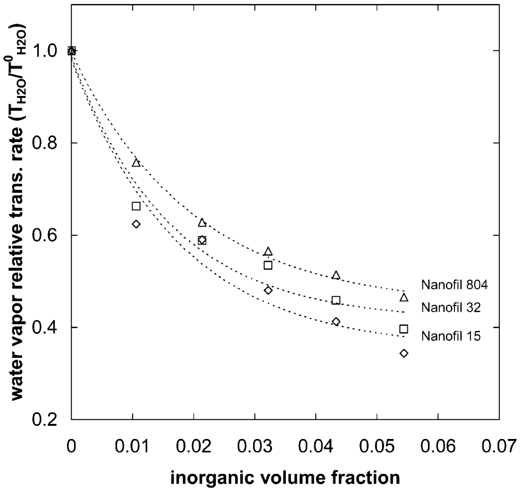

Figure 7. Dependence of the water vapor transmission rate through the PU−nanocomposites on the inorganic volume fraction. The dotted lines are guides for the eye.

Conclusions

The inclusion of small volume fractions of platelike nanoparticles in PU adhesives decreases their gas transmission rate if the interface between the two heterogeneous phases is properly designed. This can be attributed to the impermeability of the inorganic nanoparticles and the tortuous pathway the gas molecules have to cover during their random molecular motion in order to penetrate the composite. Equilibrium probably results from the attractive forces between the polymer chains and the clay organic coating or the aluminosilicate surface, retaining the polymer in the interlayer on one side and the attraction forces between the aluminosilicate layers squeezing the polymer out. This leads to exfoliation of the small particles and intercalation of the polymer chains in the large ones. Consequently, a mixture of exfoliated aluminosilicate layers and intercalated tactoids were observed in all the OM composites prepared.

The chemical structure of the clay coating and the resulting interactions with the polymer matrix strongly influences the permeation properties of the nanocomposites. Incompatibility between the phases involved may lead to a phase separation and crucial changes in the morphology of the composites, which influences the permeation properties. The incorporation of hydroxyl groups in the clay organic coating did not lead to sizable difference in the microstructure of the composite as would be expected from polymer chains tethered to the montmorillonite surface. The reaction of the OH groups of the bis(2-hydroxyethyl) hydrogenated tallow ammonium coating with the isocyanate groups could not be confirmed by IR spectroscopy. The oxygen transmission rate through the composite of this OM was also practically the same as that of the benzyl alkylammonium modification, suggesting that the OH groups did not react with the isocyanate groups. The permeation rate of water vapor through the PU−nanocomposites can strongly differ from that of oxygen. This might be due to the difference in size of the mobile units as well as to interactions of the water molecules with the matrix. WAXRD and TEM gave a qualitative picture of the microstructure of the nanocomposites but no conclusive information and a method to quantify the exfoliated and intercalated fractions of the filler is still needed.

Acknowledgment. We gratefully acknowledge financial support from TOP NANO 21 of the ETH Board and from the Swiss National Science Foundation (SNF). We also would like to thank NESTEC, Lausanne, Switzerland, and ALCAN PACKAGING, Neuhausen, Switzerland, for supporting the project. Thanks are also due to N. Matsko for the TEM micrographs.

Note Added after ASAP Posting

This article was released ASAP on 12/6/2003. In the Experimental Section, paragraph 4, sentence 5, (x_{OM}) was changed to (ρ_{OM}); paragraph 7, sentence 2, r was changed to ρ. The correct version was posted on 12/17/2003.

References and Notes

(1) Katz, H. S., Milewski, J. V., Eds. *Hand Book of Fillers for Plastics;* Van Nostrand Reinhold Company: New York, 1987.
(2) Rothon, R. N., Ed. *Particulate-Filled Polymer Composites*; Longman Scientific and Technical: Harlow, England, 1995.
(3) Alexandre, M.; Dubois, Ph. *Mater. Sci. Eng. R* **2000**, *28*, 1.
(4) Okada, A.: Usuki, A.; Kurauchi, T.; Kamigito, O. *ACS Symp. Ser.* **1995**, *585*, 55.
(5) Giannelis, E. P. *Adv. Mater.* **1996**, *8*, 29.
(6) LeBaron, P. C.; Wang, Z.; Pinnavaia, T. J. *Appl. Clay Sci.* **1999**, *15*, 11.
(7) Lee, S. *The Polyurethane book*; Wiley: New York, 2002.
(8) Wirpsza, Z. *Polyurethane Chemistry, Technology and Applications*; Ellis Horwood: New York:, 1993.
(9) Eitzman, D. M.; Melkote, R. R.; Cussler, E. L. *AIChE J.* **1996**, *42*, 2.
(10) Fredrickson, G. H.; Bicerano, J. *J. Chem. Phys.* **1999**, *110*, 2181.
(11) Gusev, A. A.; Lusti, H. R. *Adv. Mater.* **2001**, *13*, 1641.
(12) Bailey, S. W. *Reviews in Mineralogy. Blacksburg*; Virginia Polytechnic Institute and State University: Blacksburg, VA, 1984.
(13) Brindley, G. W.; Brown, G. *Crystal Structures of Clay Minerals and their X-ray Identification*; Mineralogical Society: London, 1980.
(14) Theng, B. K. G. *The Chemistry of Clay-Organic Reactions*; Adam Hilger: London, 1974.
(15) Jasmund, K.; Lagaly, G.; Eds. *Tonminerale und Tone*; Steinkopff-Verlag: Darmstadt, Germany, 1993.
(16) Osman, M. A.; Ploetze, M.; Suter, U. W. *J. Mater. Chem.* **2003**, *13*, 2359.
(17) Wang, Z.; Pinnavia, T. J. *Chem. Mater.* **1998**, *10*, 3769.
(18) Zilg, C.; Thomann, R.; Mülhaupt, R.; Finter, J. *Adv. Mater.* **1999**, *11*, 49.
(19) Chen, T. K.; Tien, Y. I.; Wie, K. H. *Polymer* **2000,** *41*, 1345.
(20) Ma, J.; Zhang, S.; Qi, Z. *J. Appl. Polym. Sci.* **2001**, *82*, 1444.
(21) Yao, K. J.; Song, M.; Hourston, D. J.; Luo, D. Z. *Polymer* **2002**, *43*, 1017.
(22) Tien, Y. I.; Wei, K. H. *Polymer* **2001**, *42*, 3213.
(23) Tien, Y. I.; Wei, K. H. *Macromolecules* **2001**, *34*, 9045.
(24) Tien, Y. I.; Wei, K. H. *J. Appl. Polym. Sci.* **2002**, *86*, 1741.
(25) Sato, H.; Yamagishi, A.; Kawamura, K. *J. Phys. Chem. B* **2001**, *105*, 7990.
(26) Vaia, R. A.; Lincoln, D. *ACS Symp. Ser.* **2002**, *804*, 99.
(27) Vaia, R. A.; Liu, W. *J. Polym. Sci., Part B* **2002**, *40*, 1590.
(28) Morgan, A. B.; Gilman, J. W. *J. Appl. Polym. Sci.* **2003**, *87*, 1329.
(29) Xu, R.; Manias, E.; Snyder, A. J.; Runt, J. *Macromolecules* **2001**, *34*, 337.
(30) Chang, J. H.; An, Y. U. *J. Polym. Sci., Polym. Chem.* **2002.** *40*. 670.
(31) Tortora, M.; Gorrasi, G.; Vittoria, V.; Galli, G.; Ritrovati, S.; Chiellini, E. *Polymer* **2002**, *43*, 6147.
(32) Grim, R. E. *Clay Mineralogy*; McGraw-Hill: New York, 1968.
(33) Crank, J. *The Mathematics of Diffusion*; Clarendon Press: Oxford, England, 1998.
(34) Lagaly, G. *CMS Workshop Lect.* **1994**, *6*, 1.
(35) Osman, M. A.; Atallah, A.; Kahr, G.; Suter, U. W. *J. Appl. Polym. Sci.* **2002**, *83*, 2175.
(36) George, S. C.; Thomas, S. *Prog. Polym. Sci.* **2001**, *26*, 985.

MA035077X